The Ottawa River Solar Observatory
Gaizauskas, V.

Publisher's version / Version de l'éditeur:

The Journal of the Royal Astronomical Society of Canada, 70, 1, pp. 1-22, 1976-02

THE JOURNAL OF THE
ROYAL ASTRONOMICAL SOCIETY
OF CANADA

Vol. 70, No. 1 | FEBRUARY 1976 | Whole No. 538

THE OTTAWA RIVER SOLAR OBSERVATORY

By V. Gaizauskas

Herzberg Institute of Astrophysics, National Research Council of Canada, Ottawa

Abstract

An observatory has been built in Canada for high resolution cinematography of active regions in the solar photosphere and chromosphere. The installation on the shore of the Ottawa River is the successor to solar facilities maintained at the Dominion Observatory from 1905 to 1970. The building, telescope, and automated control system are described with comments on the factors that influenced their design.

Introduction. The Ottawa River Solar Observatory (ORSO) was built and equipped to study the physical properties of fine-scale structures on the solar surface, particularly within active regions. The nature and origin of these features pose many unsolved puzzles. Their solutions will have broad astrophysical implications because they will reveal how the energy transported from the interior of a star is redistributed over the star's surface and throughout its atmosphere. Only in the case of the sun can we observe isolated features and isolated transient events in sufficient detail to test rigorously any theories proposed for their explanation.

Two properties of the sun are fundamental to any discussion of its surface structure. First, magnetic fields are distributed unevenly over the surface, with the strongest fields concentrated in sunspots. Secondly, immediately beneath the thin photospheric surface layer, there is a much deeper layer in which convection is the dominant factor in transporting energy outwards from the solar interior. When fluid motions occur in the presence of complex magnetic field geometries, they generate a multitude of continually changing structures at all levels of the solar atmosphere: in the photosphere, in the chromosphere, and in the corona. Granules, spicules, prominences and coronal streamers, to name only a few of the better known examples of solar structures, are products of the interplay between gravitational, magnetic, and radiation fields at different heights in the atmosphere. Our understanding of the origin and interdependence of various features is still limited owing to the complexity of the interactions between these fields of force. This limitation is especially evident in the case of the most explosive chromospheric phenomenon, the solar flare.

It is suspected on theoretical grounds that very small structures play an essential role in transferring energy in the solar atmosphere. By studying the smallest visible features, we expect that important clues will be uncovered to the mechanisms which create and support larger, long-lived features such as sunspots. The research programs at the ORSO are therefore directed towards the measurement of the properties of photospheric and chromospheric features on as fine a scale as possible with a ground-based solar telescope of modest size. This telescope has been designed specially for rapid photographic recording of solar images partly to take full advantage of the short periods when atmospheric stability at the Observatory allows the optical system to perform near its resolution limit, and partly to trace the development of the very short flash phase of chromospheric flares. Initially, simple aspects of the morphology of fine-scale structures will be studied. The capabilities of the instrument are such that more difficult measurements, on magnetic fields for example, could be undertaken in the future.

Because of its widespread influence throughout our planetary system, solar activity is a matter of great interest to other branches of astronomy and to related scientific disciplines. Research with rockets and satellites has disclosed the processes which link disturbances in the earth's magnetosphere and ionosphere with solar activity, namely, the enhanced emission of ionizing solar radiation and the enhanced injection of energetic particles into the solar wind during periods of intense solar activity. Interest in analyzing and even forecasting major solar "storms" is spurred by practical concerns over their disruptive effects on communications networks. There is also growing interest in the hypothesis that solar activity may modify, directly or indirectly, terrestrial climate and biological processes. The ORSO will therefore participate in joint studies of solar-terrestrial phenomena where its capability to detect and measure the optical properties of sporadic solar events can be used to advantage.

This paper describes the facilities at the ORSO and discusses the design of its major instrument, a photoheliograph with multiple optical systems.

Historical Background. The ORSO is a direct descendant of scientific programs launched at the turn of the century in Ottawa by the federal government. Records dating back to 1900 show that daily sunspot drawings were even then being made, probably by staff members of the embryonic Time Service, with a small telescope located near Parliament Hill. In 1905, when the Dominion Observatory came into being, a solar program began that was ambitious for its time. For its major solar instrument, the Observatory acquired a large coelostat similar to the better known Snow Telescope on Mt. Wilson (Hale 1905). Procured initially to observe the 1905 total solar eclipse in Labrador (Plaskett 1905), the coelostat was later mounted behind the Dominion Observatory in a horizontal telescope configuration that projected a solar image, 22 cm in diameter, into a spectrographic laboratory. This was the largest optical solar instrument ever built in Canada. In various modifications it was used for the spectrographic determination of the law of solar rotation (De Lury 1939), as one of the first infrared instruments to study carbon monoxide in the solar atmosphere (Locke and Herzberg 1953), and to measure the velocity field of sunspots (Rice and Gaizauskas 1973).

By 1965, it was clear that attempts to maintain the instrument at modern levels of effectiveness could never overcome the basic deficiencies of its site. The situation was aggravated by urban pressures on the use of land adjacent to the Observatory. A survey, begun in earnest that year, culminated in the selection of the Ottawa River site for the new observatory (Gaizauskas and Kryworuchko 1973). The decision to build at this location was taken in 1968, construction began a year later, and the building was finished in 1970. That year, the project was transferred to the National Research Council of Canada during a reorganization of astronomical activities in the federal government service.

The ORSO photoheliograph had its genesis around 1950 when, for chromospheric studies, the Dominion Observatory obtained a Lyot filter with a band width of 0.75 A which could be tuned to the wavelength of the Hα Fraunhofer line. Illuminated by a small refractor clamped to the barrel of the Observatory's 15-inch equatorial refractor, this device produced a monochromatic image of the entire solar disk suitable for flare detection. The automated flare patrol that developed around this basic instrument was in daily service for most of the period 1957–66. During those years, time lapse photographic records were obtained of 1800 flares and 350 other transient chromospheric events. For the final 3½ years of operation, the patrol was supported in part with funds from NASA.

The information available from the small-scale patrol images (14 mm diameter) was necessarily limited to a few elementary parameters such as the time, position, and "importance" estimates of individual events. These data were used for statistical studies of large numbers of flares, for correlations with other solar and terrestrial phenomena, and for detecting the occasional interconnection between events which were widely separated on the solar disk. Only a limited amount of physical interpretation could be applied to individual flares and other active events because the patrol image size was inadequate for the resolution of the numerous component structures of these features. A desire to overcome this deficiency gave the original impetus towards the design of the ORSO photoheliograph.

The Site. The ORSO is built on a limestone outcropping that juts out of the west bank of Lac Deschenes, a major broadening of the Ottawa River, nearly 20 km west of the centre of the city of Ottawa. Roughly 30 km^2 in area, this broad span of water is the essential factor that influences the quality of daytime seeing conditions (Gaizauskas and Kryworuchko 1973). Another name frequently used for the site location, Shirleys Bay, applies just to the portion of the river immediately south-west of the Observatory. Geographic coordinates of the site are: latitude 45° 23.'2 N, longitude 75° 53.'6 W.

The Observatory is situated in the broad and generally flat Ottawa Valley, at an elevation above mean sea level of only 58 metres. The nearest hills, about 400 metres elevation, are at a distance of more than 10 km to the north. The only direction from which air does not have an unimpeded flow over open water before reaching the site is the quadrant centred due west. Towards that side, trees and shrubs have been removed in a swath 100 metres wide between the buildings and extensive light forest and swamp. The site is a military training reserve operated by the Department of National Defence. It is reached from main highways by a service road several kilometres in length which passes through the radio-quiet site of the Communications Research Centre, Department of Communications. Although conveniently close to a city and laboratory facilities, the observatory is presently protected from encroaching urbanization by a large buffer zone which, it is hoped, will retain its natural state for many years.

Photoheliograph Design. The photoheliograph was conceived as a multipurpose solar instrument that would produce several images: of the Hα chromosphere in single active regions, of the underlying photosphere at a choice of wavelengths, and of the entire disk in Hα. Technical factors that entered into the design of the new telescope are discussed in the following sub-sections.

(a) *Spatial Resolution.* Economic considerations limited the choice of objective apertures for the new telescope to 25 cm and less. At an aperture of 25 cm, the resolution limit due to diffraction (Rayleigh criterion) is 0.65 arc-seconds for optical wavelengths at the red end of the spectrum. It is deceptive, however, to accept this figure as an indication of optical performance when the objective forms images not of isolated point sources but of a two-dimensional field covered with features having a wide range of contrasts.

In a solar image, the illumination in each elemental area is contaminated by light from overlapping diffraction patterns originating in the surrounding field. The seriousness of this effect has been discussed for the solar case by Giovanelli (1966). He has shown that even a perfect lens used during perfect seeing on an extended source will not reproduce photometric information faithfully down to the limit set by the Rayleigh criterion. In fact, an element of the image must be 6 times larger than the resolution limit if the contribution from the contaminating light originating in diffraction from adjacent points is not to exceed 20 percent. In other words, when the seeing at the ORSO is good enough to claim that features at the Rayleigh limit of the present objective are resolved throughout the solar image, the objective ought to be increased to 1.5 metre if those features are to be reproduced with a photometric accuracy of 20 percent. Atmospheric turbulence, aberrations, and residual imperfections in the geometrical figure of the telescope objective will in practice further degrade the contrast of the image.

The 25 cm objective lens chosen for the ORSO system is nevertheless a potent tool for solar research. When seeing permits diffraction-limited performance with this aperture, there is wide scope for studying the configuration of features whose sizes are near the resolution limit. Little is known as yet about the morphology of solar features with angular dimensions of one arc-second or less.

(b) *Monochromatic Observations.* The Fraunhofer lines of the visible spectrum are due to selective absorption of emergent solar radiation by numerous species of atoms and ions present in the surface layers of the sun's atmosphere. Faint lines are generally formed low in the atmosphere, in and just above the photospheric layer, whereas the strongest lines are formed higher, in more extended but rarified layers that reach up to chromospheric heights, 1000 km and more above the photosphere. The cores of strong, broad, absorption lines are formed at greater heights than the wings of the corresponding lines.

The manner in which intensity varies with wavelength across a single dark line, i.e. the line profile, can be used as a diagnostic probe of the atmosphere. A line profile indicates (i) the dominant processes responsible for the absorption in that particular line, and (ii), the physical conditions in the atmospheric regions where the absorption occurs. Profiles measured at a given point on the surface for a selection of lines belonging to the same or different atomic species can be analyzed to derive the change of physical parameters with height at that point. Variations in the profiles with time and position over the surface reveal the presence of constantly changing lateral inhomogeneities, the surface structures mentioned earlier. For many purposes, the spectroscopic analysis of these structures can be performed more efficiently by producing two-dimensional images of the surface which are monochromatic at the wavelengths of suitably chosen Fraunhofer lines. If sufficient spectroscopic resolution is available, monochromatic images can be obtained at a succession of wavelengths within a single absorption line, thus permitting a two-dimensional study of variations in the line profile.

An early instrument devised for this purpose is the spectroheliograph, a modified high dispersion spectrometer. As an image of the sun is scanned uniformly across the spectrometer entrance slit, a two-dimensional monochromatic image at the desired wavelength is built up on a photographic emulsion that sweeps past the exit slit in synchronism with the image. This powerful spectrographic tool provides high spectral purity and, as a consequence, high image contrast which aids considerably in resolving fine spatial structures. It also offers unrestricted wavelength selection in the optical range, but it suffers from low transmissivity, large size, and high cost.

Öhman (1938) and Lyot (1944) introduced an effective alternative in the form of a birefringent filter which could be inserted near the focus of a conventional telescope to produce a monochromatic image of the entire solar disk with a single short exposure. Despite its lower spectral purity, the greater transparency, compactness, and wide field characteristics of the less expensive birefringent filter have ensured its widespread acceptance in solar research, especially in flare patrols. Even the earliest filters achieved adequate spectral purity for observations in the core of the broad, flare-sensitive, Hα Balmer line. More innovative applications of the birefringent filter make use of its polarizing properties to produce simultaneously two monochromatic images at closely spaced wavelengths that can be used to detect mass motions by means of the Doppler effect (Beckers 1968) or magnetic fields by means of the Zeeman effect (Ramsey 1971).

These innovations could be adapted to the birefringent filter acquired for the ORSO telescope. However, a simpler observational goal involving two wavelength ranges will be attempted as an initial program. The chromosphere will be photographed through a narrow pass-band filter tuned to Hα while, at the same time and with the same spatial resolution, the underlying photosphere will be photographed by integrating the radiation received in a much broader wavelength band that includes Hα. The purpose of the experiment is to search for photospheric fine-structures, such as "white light" flares, that are clearly related to events occurring at chromospheric heights.

1976JRASC..70....1G

(c) *Scanning the Line Profile.* Images formed through a narrow-band filter tuned to the mean central wavelength of a strong absorption line indicate changes in absorption with time and position on the sun at that wavelength. The significance of such changes is ambiguous as long as the pass-band is left in this central position. When brightness changes occur in a feature, one cannot discriminate between: (i) symmetrical brightening or darkening of the line in that feature; (ii) a distortion-free shift of the entire line with wavelength (pure Doppler effect); (iii) asymmetrical changes in the line profile produced by physical properties peculiar to that feature, such as velocity gradients along the line of sight.

These ambiguities can be resolved by repeatedly displacing the filter pass-band in steps across the $H\alpha$ line and comparing the images secured at each wavelength. The line profile variations can thereby be examined over a two-dimensional field and over long periods of time. Features with pronounced mass motions in the line of sight are easily identified by this procedure.

Scans across the line profile can also provide limited information about the relative heights of features projected against the disk. The layers that contribute most to the formation of the wings of $H\alpha$ are situated much closer to the photosphere than the core-producing layers. However, line asymmetries are so prevalent that it is difficult to disentangle the effects of height variation and mass motion from observations in only one absorption line.

With these considerations in mind, a filter was selected for the ORSO telescope that could be tuned continuously over a range of 32 A centred on $H\alpha$. This range is more than adequate to study shifts and asymmetries in $H\alpha$; it permits tuning to weaker solar absorption lines as well.

(d) *The Effect of Parasitic Light.* The width of the wavelength band passed by a monochromatic filter relative to the width of the spectral line it isolates determines the contrast and thus the visibility of solar features which appear in that specific line. The $H\alpha$ line is naturally favoured for monochromatic photography because its full width at half maximum (FWHM), 1.2 A, is almost twice the FWHM of the transmission peaks of even the earliest commercially-built Lyot filters. The birefringent filter acquired for the ORSO telescope was built by Carl Zeiss (Oberkochen), and has the narrowest pass-band yet produced for a commercial instrument of this type, 0.25 A. In practice it is impossible to construct a perfect filter which rejects all wavelengths outside the desired pass-band. The radiation which a real filter fails to exclude, called parasitic light, is especially harmful when the filter is used for observations of absorption lines.

A birefringent filter is essentially a multiple interferometer whose operation relies on polarized rather than ordinary light. Its transmission pattern consists of many sharp peaks spaced far enough apart in wavelength to permit the isolation of one transmission window at a time with colour glass or interference filters. The transmission profile of a single peak is not rectangular; it can be approximated by a function of the form $(\sin \pi x/\pi x)^2$, i.e. it has a prominent central peak with a series of subsidiary maxima. The latter are displaced 1.5 $\Delta\lambda$, 2.6 $\Delta\lambda$, 3.8$\Delta\lambda$, ... to each side of the central peak whose FWHM is $\Delta\lambda$. The corresponding intensities of the subsidiary maxima are 0.047, 0.016, 0.008, ... of the central peak intensity. When the central peak is tuned to the core of the Hα absorption line, successive subsidiary maxima transmit radiation from progressively brighter portions of the line intensity profile. The radiation transmitted in the sidebands is therefore greatly enhanced relative to that transmitted in the central peak and serves to reduce contrast. The enhancement diminishes as the filter is tuned away from the absorption minimum and is negligible at displacements greater than $\pm$ 0.7 A. The sidebands produce, in effect, weak, overlapping solar images representative of layers successively closer to the photosphere for increasingly remote maxima. In addition to degrading the contrast of features on the disk, the parasitic light produces false intensity gradients at the solar limb which have been subject to misinterpretation (White and Bhavilai, 1970). The seriousness of the problem is apparent in the following examples. The 0.25 A birefringent filter supplied by Zeiss with a 60 A bandpass prefilter produced images at the centre of Hα with a 38 percent content of parasitic light originating in discrete sidebands and a very weak background leaked over a broad wavelength range. For the Sydney ⅛ A birefringent filter, the Hα images were found by Beckers (1964) to have a 58 percent content of parasitic light due to similar causes.

In order to improve the contrast of images at the centre of Hα, and therefore the ability to detect fine structures, the sidebands must be suppressed by using a prefilter with a narrower pass-band. A decrease of this bandwidth by 10 times has been adopted in the ORSO system and it results in a minor reduction in the parasitic component in the Hα images to 31 percent. The full tuning range of the birefringent filter can still be achieved, when necessary, by tilting the 6 A interference prefilter in the beam. A major reduction in the parasitic light, to 5 percent or less at Hα, requires a narrowing of the prefilter pass-band by another factor of 10, to about 0.6 A. This is technically feasible but, when the resultant images are photographed, exposure times may increase so much on account of transmission losses in the prefilter that practical application of the filter combination may be restricted to brief periods of ideal observing conditions (for example, see Loughhead and Tappere, 1971).

(e) *Cinephotography*. Changes in photospheric granulation patterns are detectable within several minutes. Running penumbral waves and bright umbral flashes (Giovanelli 1972; Zirin and Stein 1972) seen in Hα recur at intervals of about 250 and 160 seconds respectively. Some flares erupt to peak Hα brightness in seconds. At the other extreme, filaments persist for hours or even days with only gradual changes in their shapes. Time lapse photography is indispensable for the study of features over this entire range of lifetimes. Any event can be subsequently displayed to the best advantage for its analysis by using variable time compression of the original film record.

Four 35 mm cine cameras are available for use at different locations within the ORSO telescope. They can take exposures at rates which are continuously adjustable up to two frames per second. Exposure times are adjustable over a range which depends upon the particular camera and its application; ¼ second and 5 milliseconds are extreme limits.

(f) *Automation.* The highly intricate patterns formed in the solar atmosphere change in times measured in minutes or even seconds. Fluctuations in seeing, however, distort solar images formed by a ground-based telescope in shorter times which are typically much less than a second. The distortions may be too pronounced and persistent for the full resolution of the telescope to be realized. Experience shows that favourable days occur at the ORSO when seeing is above average for many minutes at a time. There is then a great increase in the likelihood of securing images with definition at the limit of resolution for a 25 cm objective. During such prolonged periods, which recur randomly throughout the best days, excellent optical definition frequently occurs in momentary bursts lasting about one second. Because solar radiation is so intense, very high rates of data acquisition can be used to ensure that cameras are exposed during as many of these bursts as possible. The accumulation of data at an accelerated rate is particularly worthwhile for the study of small-scale structures whose lifetimes are shorter than the prolonged periods of above-average seeing.

Owing to the unpredictability of changes in seeing, and of the passage of clouds as well, a ground-based telescope will be used more effectively if its rate of sampling data is controlled automatically. Provision has therefore been made to monitor, by photoelectric means, the sharpness and brightness of the solar image formed by the ORSO telescope. The electrical signals produced by the monitors select the observing rate automatically. The same control will be exercised over several telescopes operating independently of each other within the framework of the photoheliograph by using a minicomputer. The major advantage arising from this approach to the control of the system is that complex sequences of mechanical operations can be altered simply and rapidly by making changes in software in order to satisfy the requirements of different observing programs.

(g) *Photoelectric Guiding.* The advantages of cinephotography cannot be realized unless the telescope continuously tracks the sun with sufficient precision for the smallest resolved features to appear frozen in position during cine projection. The guider was designed therefore to hold the solar image to within 0.5 arc-seconds (rms) for extended periods of several hours assuming perfect seeing, constant wind loading, and negligible telescope flexure. Other design goals included freedom from temperature drift over the range $-20°$ to $+35°$C, insensitivity to sky transparency changes over a range of 4:1, and retention of control when clouds block only a portion of the image. A system meeting all these requirements was designed in consultation with Spar Aerospace Products Limited of Toronto, Ontario.

(h) *Mechanical Configuration.* It is advantageous to have independent optical systems so that observations can be made simultaneously of the same solar region or different regions as desired. The separate systems could be mounted on one stationary base and illuminated by one or more coelostats or heliostats. This approach, although attractive from the point of view of stability and rigidity, was rejected in order to avoid problems with image rotation, variable instrumental polarization, and the higher level of scattered light normally encountered in reflectors compared to refractors. It was decided instead to attach the individual optical systems to a single equatorially-mounted platform that tracks the sun like a conventional telescope. This decision was prompted by the success of the 'spar' telescope designed by Carroll (1970) for operation without the protection of a dome or other housing at the Lockheed Solar Observatory. Carroll's compact design encloses all optical paths, lends itself readily to internal thermal control, yet provides quick access to all components for adjustment and cleaning.

The initial adaptation of this design to the conditions envisaged at the ORSO was planned in consultation with Mr. Carroll. Detailed design was performed under contract with Spar Aerospace Limited.

Description of the Photoheliograph. The main frame of the photoheliograph consists of a welded steel cruciform structure, 3.5 m long, which provides 8 flat mounting surfaces for optical benches (figure 1). Removal and insertion of optical components is simplified by attaching them with quick-release clamps to dovetail tracks which are bolted to the flat surfaces defined by the strutwork. Eight hinged aluminum panels enclose the entire spar in a cylindrical shell 0.8 m in diameter and permit convenient access to the interior. This shell is insulated and lined with flexible heating panels for warming the interior during winter nights. During observing periods, the heaters are switched off while small fans mounted on the rear bulkhead

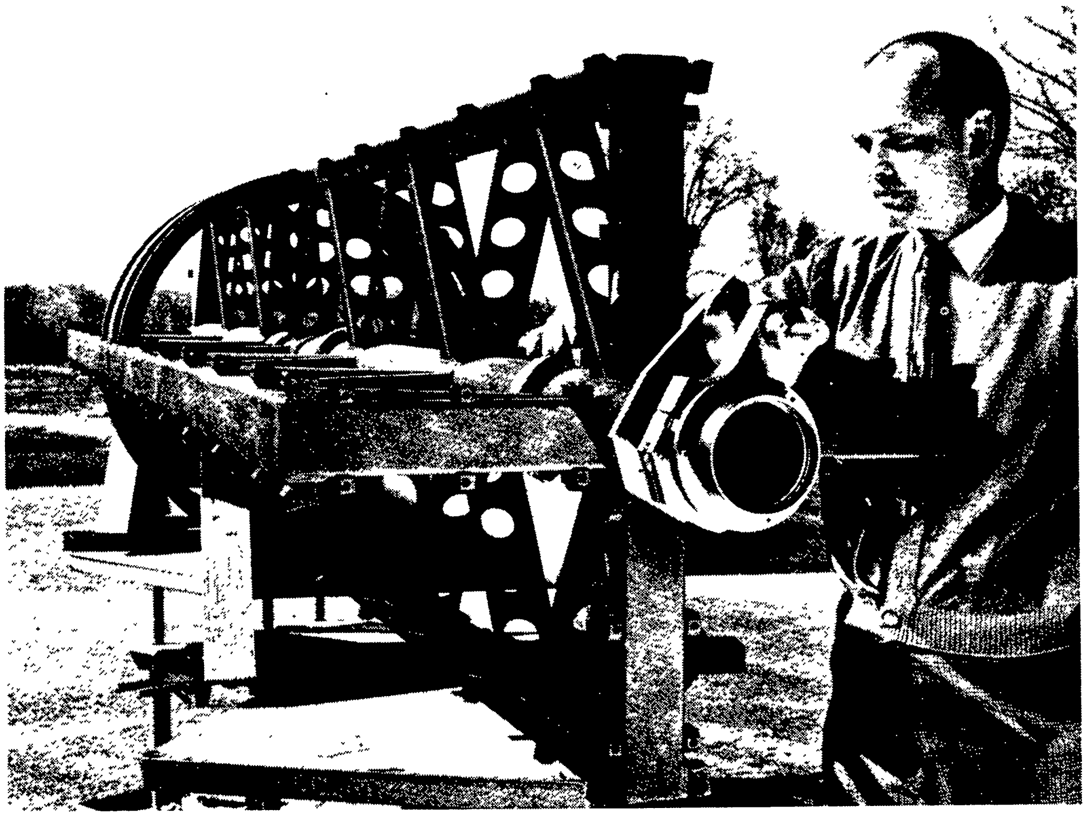

FIG. 1—Internal strutwork, or spar, of the ORSO photoheliograph. Only the central guiding telescope was installed at this stage of construction.

draw warm air out of the telescope. The spar is fork-mounted on a polar axis driven by a double chain and sprocket instead of the conventional worm and gear for the final reduction stage (Carroll 1970). The declination travel is restricted to the annual solar range in order to keep the fork arms short and rigid. Fine adjustment in declination over a range limited to one solar diameter is accomplished by using an eccentric cam to displace a tangent arm fixed to the declination axis. The declination axis of the assembled telescope is more than two metres above the observing floor. The mechanical shell of the telescope, excluding all optics and electrical controls, was fabricated by Canadian Westinghouse Limited at their Hamilton, Ontario plant.

The optical system that produces the dual images for simultaneous photography on a large scale of the Hα chromosphere and photosphere is housed in the two upper quadrants of the spar. The south-west quadrant holds an evacuable refractor with an aperture of 15 cm for wide band photography of the photosphere. In the south-east quadrant there will be a telescope of 11 cm aperture for photographing the entire solar disk at Hα as a supplement to the large scale observations.

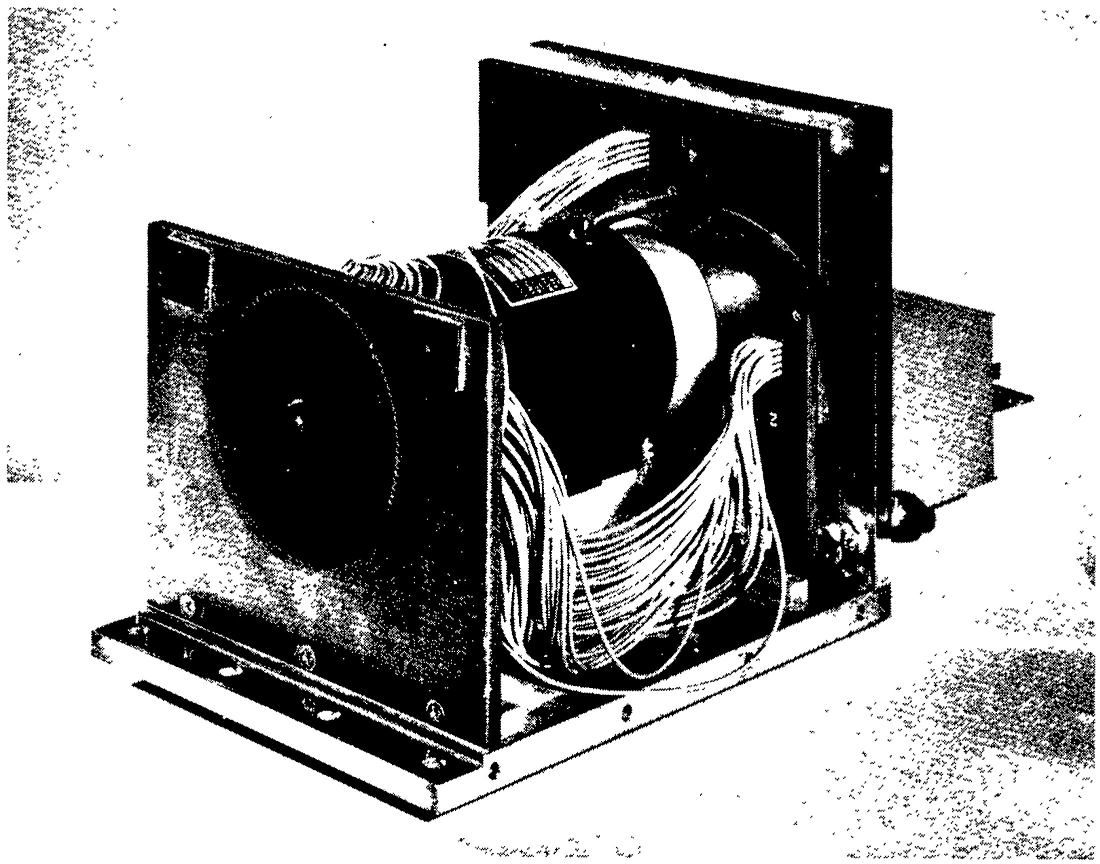

FIG. 2—Device for measuring image motion with the ORSO guiding telescope. Electronic components for the guider are carried on board the telescope.

A tube 12 cm in diameter centred in the spar framework carries a smaller telescope to form an image for photoelectric guiding purposes. The guidance system keeps the central axis of the spar locked on the centre of the sun at all times. The small patrol telescope will be collimated to the same axis. For the other telescopes, images are located independently by motorized displacements of intermediate components in their optical trains.

The guiding telescope, a compound refractor with an 11 cm aperture, produces a full image of the sun 9 cm in diameter at the rear bulkhead of the spar. An intermediate relay lens is translatable over a small range to keep the image diameter constant despite the annual change in the sun's angular diameter. The entire compound refractor is displaced as a unit to focus the final image in the plane of a narrow annulus whose inner diameter exactly matches the image. Behind the annulus, an opaque sector spins about an axis coincident with the optic axis (see figure 2). Any light passed from the solar limb through the annulus is directed by fiber optics to four silicon photovoltaic cells which collect the flux from four quadrants in the four cardinal directions. When the image is exactly centred on the rotation

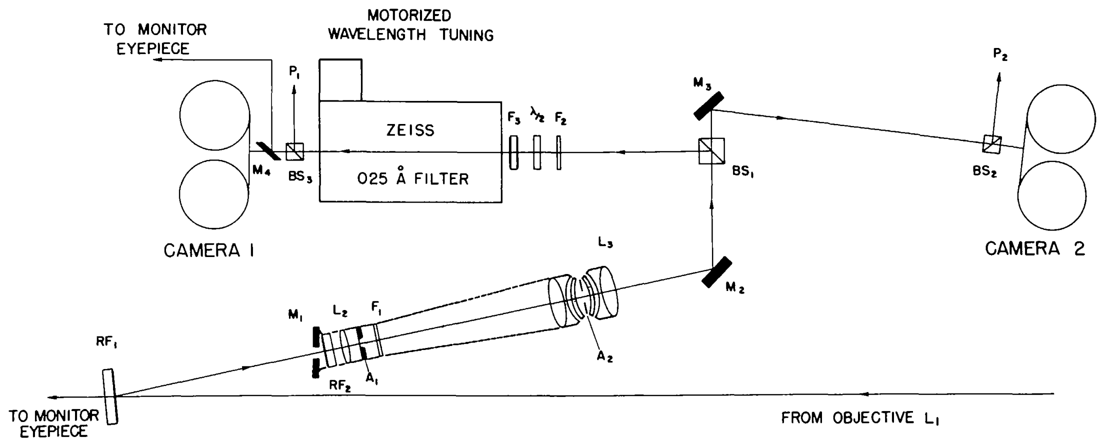

FIG. 3—Optical schematic of the dual-image Hα telescope. Designations of components are explained in the text.

axis, the outputs of opposite pairs of photocells are equal. A minute displacement of the telescope creates a difference between the outputs from opposite photocells. The subtracted outputs are modulated at the frequency of rotation of the sector. The magnitude and direction of the shift determine the amplitude and phase of the alternating error signals. The determination of the phase of the error signal is greatly simplified by using a polarized synchronous motor to spin the sector. Because the motor shaft always assumes the same orientation with respect to the AC line voltage, phase reference can be derived from the line voltage itself. The telescope's position is corrected by applying the amplified error signals to servomotors coupled to the hour angle and declination axes.

The dual-image telescope for high-resolution photography, illustrated schematically in figure 3, is the most elaborate optical system in the photoheliograph. The beam from the 25 cm objective, an air-spaced doublet, is intercepted before it forms an image by RF_1, a multilayer dichroic filter coated as a high efficiency reflector for wavelengths near Hα. Yellow-green light transmitted by RF_1 forms an image at an eyepiece for identification of active regions and visual estimation of seeing. Only the portion of the red beam reflected by RF_1 that eventually forms the images of the desired solar region passes through the reflecting diaphragm M_1. Before it comes to a focus in the plane of a fine wire reticle at A_1, the constricted beam is filtered in order to absorb infrared radiation and to narrow further the wavelength range to a band several hundred Angstroms broad at Hα.

Field lens L_2 images the objective L_1 in the plane of the iris diaphragm of relay lens L_3 so that each point of the objective contributes to the formation of the final image without vignetting when the iris is fully opened. The lens L_3 enlarges the primary image diameter from 4 to 13 cm. The assembly comprising L_3 and the components near the prime focus is attached as a single unit to an X-Y translation stage. Stepping motors coupled to the translation screws are actuated by push buttons or the computer to displace the assembly and hence the optic axis of the enlarging system. In this way, the final images of the desired solar region are located precisely within the film gates of the cine cameras. Upon emerging from L_3, the beam is reflected by mirror M_2 into the adjacent quadrant of the spar where it is divided by the polarizing beamsplitter BS_1 into two beams, equally intense but plane polarized in mutually orthogonal directions. The use of fully polarized beams reduces intensity losses at the birefringent filter.

The beam reflected by BS_1 passes through a half-wave plate which aligns the beam's polarization vector with the polarizer at the entrance to the Zeiss birefringent filter. The etalon of the 6 A bandwidth prefilter F_3 is enclosed in a thermally controlled chamber attached to the faceplate of the Zeiss filter. The optical elements of the birefringent filter are immersed within an oil bath whose temperature is held constant within $\pm$ 0.03°C in order to hold the pass-band of the filter at the wavelength of Hα. The narrow bandwidth beam emerging from the Zeiss filter is restricted in diameter to 26 mm, the diameter of the last element in the filter. Before it reaches the film plane in camera 1, a portion of this emergent beam is directed via beamsplitter BS_3 to photocell P_1 whose electrical output controls the shutter opening in camera 1. Control of the exposure time is essential to compensate for changes in intensity as the Hα line is scanned in wavelength and for fluctuations in sky transparency. Mirror M_4 reflects the beam into a viewing periscope for visual alignment and focusing, but is withdrawn when filming is in progress.

The beam transmitted by BS_1 is reflected by M_3 to cine camera 2 where it forms an image of the photosphere with an effective bandwidth of 400 A centred near Hα. Before reaching camera 2, this beam is intercepted by another beamsplitter BS_2 so that a faint image is formed in the plane of a scanning pinhole at P_2. This auxiliary device, still under development, will sense image contrast and will serve as an electronic monitor of image sharpness. The grid formed by fine wires at A_1 permits a precise superposition of the images photographed with cameras 1 and 2.

Automatic Control and Data Acquisition. The control system can perform the following tasks: automatically control repetitive mechanical operations within the photoheliograph; continuously sample and record on magnetic tape the outputs of sensors responding to image quality, image brightness, guiding errors, and local microthermal fluctuations; sequentially sample and record on magnetic tape the outputs of sensors that measure temperatures inside the telescope and wind parameters; indicate malfunctions and halt operation in specific cases where intervention by the observer is required; and allow interaction of the observer with the system at any time via teletype to alter operating conditions which have been specified in advance in the software. The system was built under contract with Digital System Associates Ltd. and Digital Methods Ltd. of Ottawa. The heart of the system is a DEC PDP-8L processor.

Experience in observing the development of different solar features makes it possible to define the optimum rate of taking exposures in terms of the quality of the images. Specific values of the electrical outputs of the sensors that monitor the sharpness and brightness of the solar image are then defined as the threshold levels where the cine cameras change their filming rates. These values are entered into the processor's memory as tables, one table for each camera. The entries can be changed at will by the observer to provide the most suitable combination for a particular observing program. The brightness of the Hα image, for example, will be strongly affected by the presence of a major flare. When observations of flares are of paramount importance, the brightness factor can be given priority to accelerate the exposure rates, even during mediocre seeing. The exposure rate for each camera changes independently of those of the others whenever a threshold level is crossed. As conditions degrade, the interval between exposures increases in the sequence 1, 2.5, 5, 10, and 25 seconds.

A similar procedure is followed to set up the wavelength scans. The Zeiss filter is tunable at the rate of 0.44 A per second over the range H$\alpha \pm 16$ A by rotating a single shaft with a stepping motor under the control of the processor. A single command transmitted by the observer through a teletype will cause the motor to shift the pass-band of the filter in a sequence of steps (which need not be uniform) across the Hα line profile; camera 1 takes an exposure at the completion of each shift. The pattern of wavelength steps is determined by another table of entries stored in the processor's memory. The number of entries in that table specifies the number of wavelength steps (up to 40) that are made in a single scan across the line. Individual entries specify the duration (up to 1 second) of the pulse train sent to the stepping motor to make one wavelength step. The pattern of steps is normally arranged to be symmetrical about the centre of Hα.

Building. The building includes a telescope shelter, control room, observing platform, and darkroom, all arranged for convenience on a single floor supported by steel columns. The control room, located at the north end of the structure, houses the auxiliary electronic equipment. The telescope base is fixed to a solid concrete pier nearly 5 m high. In mid-summer, the objective lenses reach a maximum height of 10 m above grade. The central portion of the building opens in two halves that roll back north and south to expose a large unobstructed area, 4.5×13 m, around the telescope (see figure 4). A steel grating floor in this area provides ventilation around the telescope base but is covered with panels of aluminum treadplate during severe weather conditions. An unusual feature of the design is the mating of the sides of the building along a 45° incline in order to increase the effectiveness of the building as a wind screen during observations. When the building is partially opened, the inclined gap between its halves describes the angular band occupied by the sun in its diurnal passage during the equinoxes. The general contractor for the construction of the building was Cyrus J. Moulton Ltd. of Manotick, Ontario.

White paint has been applied over the entire steel structure to minimize solar heating. Crushed white dolomite has been spread underneath the building for the same reason. At the height of the spring run-off, the river almost reaches the fence surrounding the building (figure 4), but by late summer it has dropped 2 metres or more.

A weather tower, 10 m high and 20 m north of the building, supports a bivane anemometer and two fast-response thermistors. These sensors are monitored from the control room for an indication of local micrometeorological conditions.

Performance. All design goals for the guider have been realized in practice. The AC detection system, inherently insensitive to temperature drifts, has operated for several years with only occasional maintenance. As reported by Carroll (1970), the sprocket and chain drive produces smooth tracking. A periodic error with a peak-to-peak amplitude of 0.7 arc-seconds and a one minute period has been traced to the worm gear reducer that precedes the sprockets. Tracking performance deteriorates noticeably in gusty conditions once the wind speed exceeds 2 metres/sec (~ 5 mph). When partially opened, the building makes an effective windscreen. However, adverse effects on the seeing due to turbulence around the building are then so pronounced that observations are conducted with the building in this condition only as a desperation measure on very windy days (speeds exceeding 10 metres/sec).

Seeing is best when a steady breeze blows across the fully opened building, usually from the direction of the river, at times from the land side. The time at which the best seeing occurs varies from day to day. Noon is generally favoured, but long periods of excellent seeing have been experienced at 4 and even 5 hours before or after local noon. The months between May and October have the best seeing conditions.

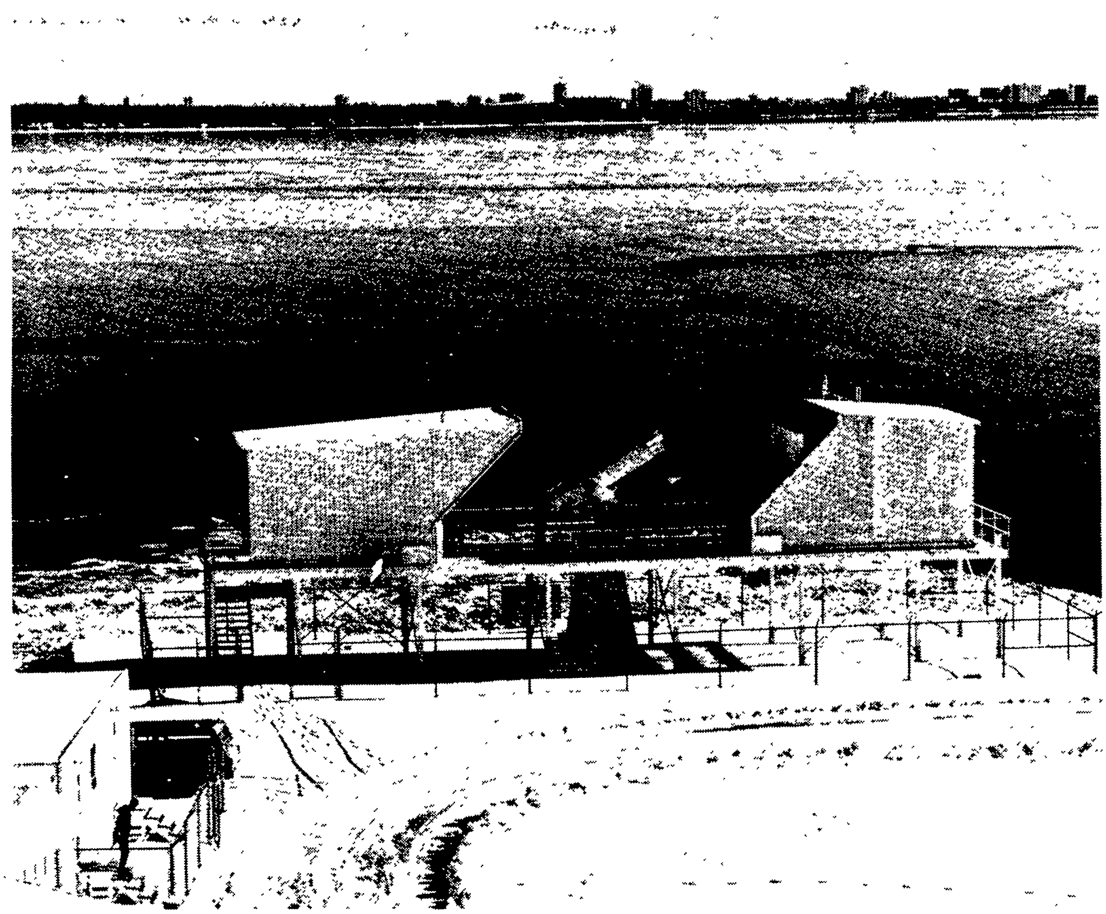

FIG. 4—Aerial view of the ORSO, December 1973, looking eastward to Ottawa. The distance across the river to the shore below the apartment towers near the centre of the skyline is 8 km. Beginning in late December, the river freezes over for four months.

Temperature changes of the telescope interior cause a gradual drift in the location of the primary focal plane. The enlarging optics magnify this effect without introducing additional drifts unless diurnal temperature changes are abnormally large. Automatic focus adjustment will be incorporated into the control system to prevent the loss of good data owing to thermal problems.

Examples of the optical performance are shown in figures 5, 6 and 7. All exposures have been made on Kodak SO-392 emulsion. The grid formed by the reticle wires consists of squares 10^5 km to a side on the solar surface; the width of a wire corresponds to nearly 900 km. A group of young, rapidly developing spots located near disk centre is depicted in figure 5. Seen in the core of Hα, the spots are embedded in a bright plage crossed by two sets of roughly parallel dark filaments. The set of filaments adjacent to the spot near the centre of the frame appears with the very ends of the

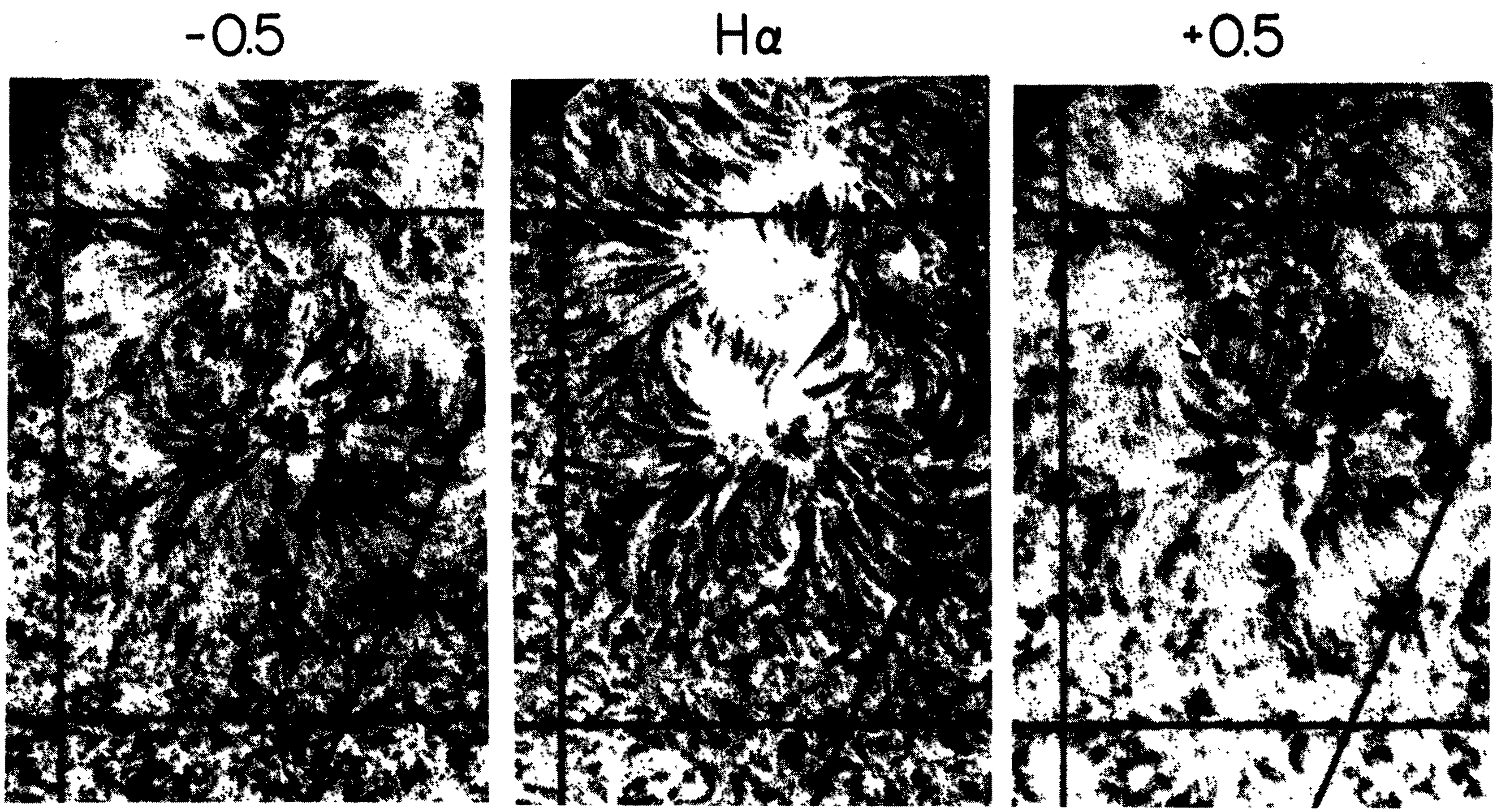

FIG. 5—Monochromatic images selected from a single scan across Hα of a young spot group, Mt. Wilson No. 19235, 5 August, 1973. Positive wavelength displacements, measured in Angstroms, are made towards the red wing of Hα. The white arrow in the red wing photograph points to several dark knots located at the ends of filaments which appear in the central Hα image as a cluster of nearly parallel strands. The absence of the knots in the blue wing photograph, taken 40 seconds later, indicates descent towards the solar surface of the material in those portions of the filaments.

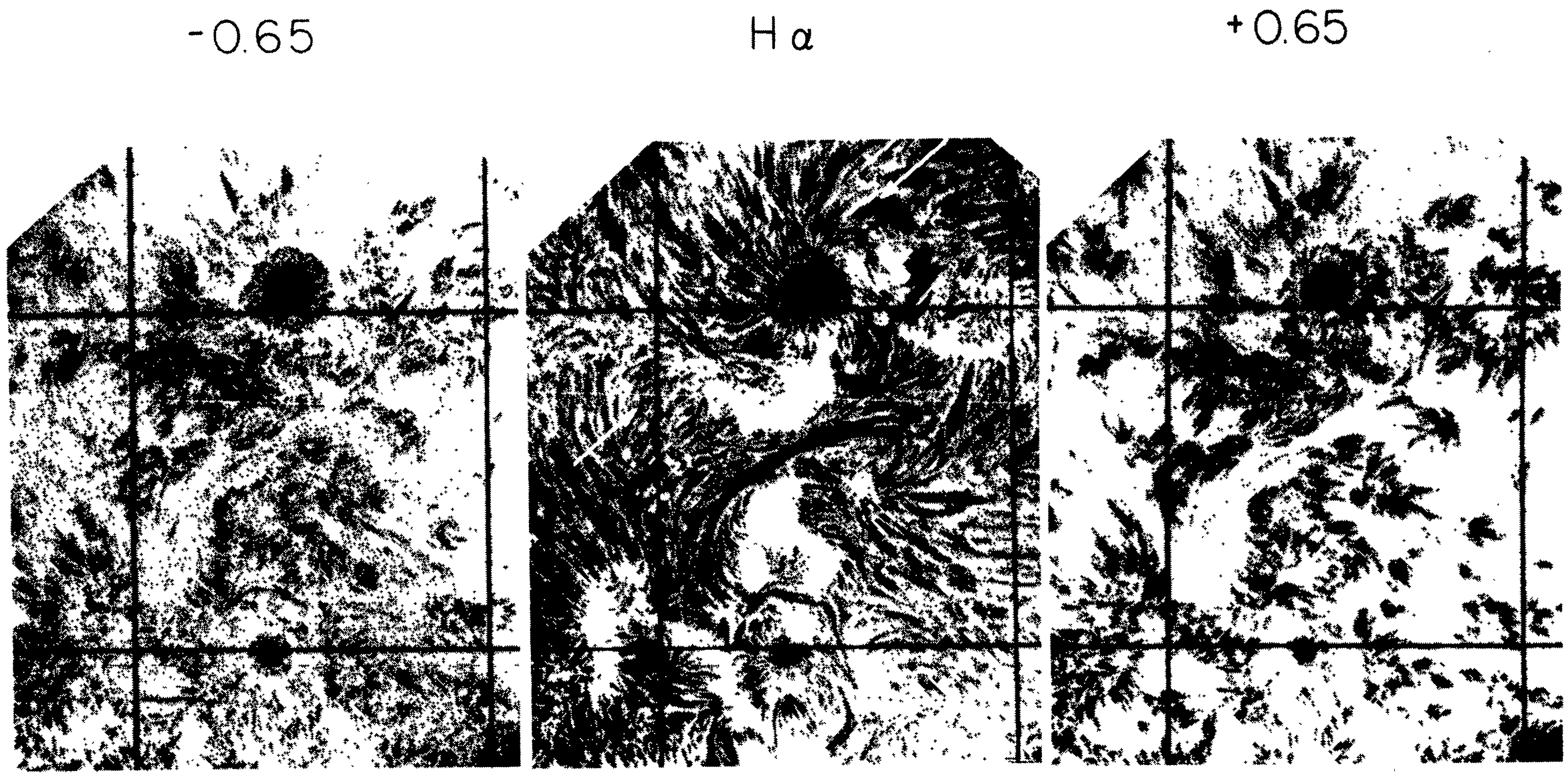

FIG. 6—Monochromatic images selected from a single scan across Hα of a long-lived sunspot, Mt. Wilson No. 19448, 10 August, 1974. The white arrows in the central Hα photograph point towards the bright arc of a penumbral wave traversing the penumbra of the upper sunspot. The wave front is not visible in the wing photographs.

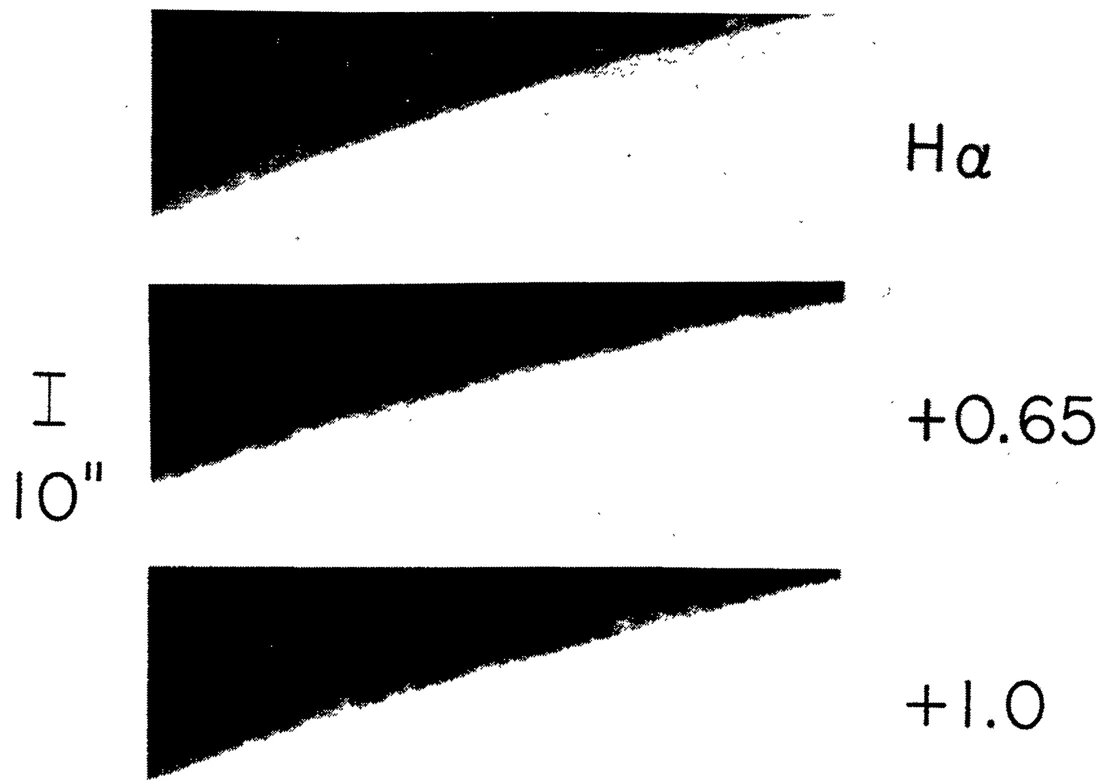

FIG. 7—Monochromatic images selected from a single scan towards the red wing of Hα of a quiet region of the limb, 10 May, 1975. In order to reveal the faint spicules at the limb in these photographs, the solar surface has been heavily overexposed.

filaments more strongly enhanced, relative to the inter-connecting strands, in the red (positive wavelength displacement) than in the blue wing. A similar, less pronounced effect is discernible in the filament set crossed by the upper horizontal wire. The filaments are evidently arches in which material drains down both legs of each arch. Such filament patterns, characteristic of the earliest stages of growth of sunspot groups, are called arch filament systems (AFS) by Bruzek (1969) and emerging flux regions (EFR) by Zirin (1972). Excellent seeing during the blue wing exposure reveals numerous dot-like features at the theoretical resolution limit in areas underlying the bright plage and in the "quiet" chromospheric background near the lower horizontal wire.

By way of contrast, a mature spot is illustrated in figure 6. From the multitude of fine structures seen in these images, two are worthy of special attention. Centred on the 10 o'clock position in the penumbra of the larger spot in the central Hα image, there is a bright arc bounded on both sides by dark bands in the system of radial penumbral filaments. Seen in cine projection, alternate bright and dark bands propagate outwards from the edge of the umbra with a repetition rate near 4 minutes, for a while in one sector of the penumbra, then in another. This phenomenon, the running penumbral wave (Giovanelli 1972, Zirin and Stein 1972), can be detected in single, regular sunspots only under the very best seeing conditions. The other feature of note is the ring of bright dots surrounding both spots, especially pronounced in the blue wing image. Dot size is limited by the telescope resolution. Dot visibility peaks at wavelengths just under 1A from line centre. Dot lifetimes, intensity variations, proper motions, etc. have yet to be determined. These features appear to be distinctly different from the better known "Ellerman bombs"; they resemble the "bombs" in scale but not in their explosive behaviour.

The performance of the telescope for the investigation of limb features is illustrated in figure 7. In the core of Hα, the limb is encircled by a faint narrow band, about 6000 km wide, with a smooth inner edge and a highly ragged outer boundary. As the filter is tuned out to either wing of Hα, the diffuseness of this limb band resolves at displacements near 1 A into numerous fine *spicules* of varying brightness, lengths, and inclinations to the limb. The properties of these features and their significance to the structure of the chromosphere and corona have been summarized by Beckers (1972). The sharp "inner limb" seen at line centre is an instrumental artifact. The step-like change in intensity is produced by light from the wings of Hα leaked by the innermost sidebands of the Zeiss filter as discussed in the section on parasitic light. The limb seen in the wing photographs is the true limb for those wavelengths.

Acknowledgments. A project of this magnitude could not be conceived or accomplished without the cooperation of many agencies and individuals. Besides the sponsoring agencies, the following government departments and branches have contributed to the location, design, construction and operation of the ORSO: Department of National Defence; Communications Research Centre, Department of Communications; Property, Planning and Management Division, Department of Energy, Mines, and Resources (DEMR); Department of Public Works; Radio and Electrical Engineering Division (REED), National Research Council (NRC).

Strong support in the initial planning stages by Dr. J. H. Hodgson, then Director of the former Observatories Branch, DEMR, ensured the commencement of the project. Since 1970, similar backing by Dr. J. L. Locke, Director of the Herzberg Institute of Astrophysics, NRC, has made it possible to bring the ORSO into operation at the designed level of performance.

Numerous suggestions that were incorporated into the completed telescope originated with G. A. Carroll and H. E. Ramsey, Lockheed Solar

Observatory, and G. A. Brealey, Dominion Astrophysical Observatory. Many of the auxiliary telescope fittings were designed by D. B. Hoey of REED. All telescope fittings and modifications were fabricated by the Model Shops of REED; the efforts of D. W. Johnson and A. R. Taylor in this phase of the project are gratefully acknowledged.

The telescope and control system were made operational with the active participation of Dr. L. W. Avery, S. A. Gardiner, and A. Kryworuchko. Special recognition is due Aren Groen, not only for the installation and interconnection of all electronic components in the Observatory, but for the design and development as well of many special-purpose circuits. The successful operation of the ORSO is due in no small measure to his skill and diligence.

References

Beckers, J. M. 1964, *A Study of the Fine Structures in the Solar Chromosphere*, Ph.D. Thesis, AFCRL–64–770, Environmental Research Paper No. 49.
Beckers, J. M. 1968, *Solar Phys.*, **3**, 258.
Beckers, J. M. 1972, *Ann. Rev. Astron. and Astrophys.*, **10**, 73.
Bruzek, A. 1969, *Solar Phys.*, **8**, 29.
Carroll, G. A. 1970, *Sky and Telescope*, **40**, 10.
DeLury, R. E. 1939, *J.R.A.S. Canada*, **33**, 345.
Gaizauskas, V. and Kryworuchko, A. 1973, *J.R.A.S. Canada*, **67**, 217.
Giovanelli, R. G. 1966, *Proceedings of the Meeting on Sunspots (Florence)*, Vol. II, Tome 2, p. 74.
Giovanelli, R. G. 1972, *Solar Phys.*, **27**, 71.
Hale, G. E. 1905, *Ap. J.*, **21**, 151.
Locke, J. L. and Herzberg, L. 1953, *Can. J. Phys.*, **31**, 504.
Loughhead, R. E. and Tappere, E. J. 1971, *Solar Phys.*, **19**, 44.
Lyot, B. 1944, *Ann. d'Astrophys.*, **7**, 31.
Öhman, Y. 1938, *Nature*, **141**, 157 and 291.
Plaskett, J. S. 1905, *Report of the Chief Astronomer*, Department of the Interior (Ottawa).
Ramsey, H. E. 1971, *Solar Phys.*, **21**, 54.
Rice, J. B. and Gaizauskas, V. 1973, *Solar Phys.*, **32**, 421.
White, O. R. and Bhavilai, R. 1970, *Astrophys. Letters*, **5**, 137.
Zirin, H. 1972, *Solar Phys.*, **22**, 34.
Zirin, H. and Stein, A. 1972, *Ap. J. Letters*, **178**, L85.